

LETTER TO THE EDITOR

On the nature of X-Ray Flashes in the SWIFT era

B. Gendre^{1,2}, A. Galli^{1,3} and L. Piro¹

¹ IASF-Roma/INAF, via fosso del cavaliere 100, 00133 Roma, Italy

e-mail: gendre@iasf-roma.inaf.it, galli@iasf-roma.inaf.it, piro@iasf-roma.inaf.it

² Universit degli Studi di Milano - Bicocca - Piazza dell'Ateneo Nuovo, 1 - 20126, Milano

³ INFN-Trieste, Padriciano 99, 34012 Trieste, Italy

Received —; accepted —

ABSTRACT

Aims. X-Ray Flashes (XRFs) are soft gamma-ray bursts whose nature is not clear. Their soft spectrum can be due to cosmological effects (high redshift), an off-axis view of the jet or can be intrinsic to the source. We use SWIFT observations to investigate different scenarios proposed to explain their origin.

Methods. We have made a systematic analysis of the afterglows of XRFs with known redshift observed by SWIFT. We derive their redshift and luminosity distributions, and compare their properties with a sample of normal GRBs observed by the same instrument.

Results. The high distance hypothesis is ruled out by the redshift distribution of our sample of XRFs, indicating that, at least for our sample, the off-axis and sub-energetic hypotheses are preferred. Of course, this does not exclude that some XRFs without known redshift could be at high distance. However we find that taking into account the sensitivity of the BAT instrument, XRFs cannot be detected by SWIFT beyond ≈ 3 . The luminosity distribution of XRF afterglows is similar to the GRB one. This would rule out most off-axis models, but for the homogeneous jet model. However this model predicts a GRB rate uncomfortably near the observed rate of supernovae. This implies that XRFs, at least those of our sample, are intrinsically soft.

Key words. X-ray: flashes—Gamma-ray: bursts

1. Introduction

A new class of “soft Gamma-Ray Burst (GRB)” making up about one third of the total population of GRBs was discovered by BeppoSAX (Heise et al. 2001). An observational classification based on the hardness ratio of the prompt emission divides GRBs in : the classic hard GRBs, the soft X-Ray Flashes (XRFs), and an intermediate class of X-Ray Rich (XRR) events (Lamb & Graziani 2003; Barraud et al. 2003). In term of their spectral behaviors, XRFs showed a shape similar to the GRB one, with the only difference that the energy at which the νF_ν spectrum peaks (the peak energy, E_p , see Band et al. 1993) has a lower value (Sakamoto et al. 2005; D’Alessio et al. 2006). They fulfill the so-called Amati relation (Lamb et al. 2005).

Three scenarios have been proposed to explain the origin of XRFs. The high redshift scenario (Heise et al. 2001) appeared to be the most straightforward explanation for these events. In fact, a normal GRB placed at a redshift of 7-8 would be observed as an XRF due to the cosmological effects (D’Alessio et al. 2006). Thus, the softness of XRFs could be only an observational bias due to distance.

The off-axis scenario is based on the assumption that we observe normal GRBs in (or very nearby to) the axis of the jetted fireball that produces the burst, while XRFs are observed off-axis. Several models, assuming different jet structures, have been proposed to account for the soft spectrum of XRFs (Yamazaki et al. 2002, 2003, 2004; Lamb et al. 2005; Zhang et al. 2004; Eichler & Levinson 2004; Toma et al. 2005).

Finally, the soft spectrum of XRFs could be due to an intrinsic property of the source (e.g. a sub-energetic or an inefficient fireball), that would radiate most of its energy in the X-ray band rather than in the gamma-ray one (Dermer 1999; Barraud et al. 2005; Ramirez Ruitz & Lloyd-Ronning 2002).

In a previous work using the BeppoSAX observations, D’Alessio et al. (2006) have tested the distant event and off-axis observation hypotheses. Their main conclusion was that the dataset they had in hand gave little support to the high distance scenario. In fact, the measured redshifts of a few XRFs ruled out the hypothesis that all of them are distant events, thus calling for an alternative explanation for nearby events. Under the assumption that GRBs and XRFs in their sample were at the same average distance, D’Alessio et al. (2006) showed that a jet observed off-axis could marginally explain the data. However, they recognized that their findings need to be verified with an adequate sample of events with known redshift and therefore with a known luminosity distribution.

The purpose of this letter is to further investigate the XRF nature, taking advantage of the larger sample of event with known distance available in the SWIFT era. We present the sample and the data analysis in section 2. While not all XRFs are distant events, some could be. We investigate the possible existence of distant events in section 3. Using the luminosity distribution of XRFs, we discuss off-axis models in section 4. We finally summarize our findings and conclude in section 5. In the following, we use a flat universe model ($H_0 = 73$, $\Omega_m = 0.23$).

Table 1. SWIFT XRF sample. We report the redshift, the prompt spectral parameter β , the 2.0-10.0 keV flux 40 ksec after the burst (observer frame) and the 2.0-10.0 keV luminosity 20 ksec after the burst (rest frame).

XRF name	Redshift	β	X-ray flux 10^{-13} erg s $^{-1}$ cm $^{-2}$ (40 ksec, observer frame)	X-ray luminosity 10^{44} erg s $^{-1}$ (20 ksec rest frame)
060512	0.4428	2.49	0.9	0.1
060218	0.033	2.5	1.9	0.00071
060108	2.03	2.01	3.2	12.3
051016B	0.9364	2.38	6.8	4.2
050824	0.83	2.78	5.2	2.1
050416A	0.6535	3.20	6.0	1.6
050406	2.44	2.44	0.57	3.6
050319	3.24	2.38	20.0	201
050315	1.949	2.11	29.0	107

2. Data reduction, analysis and results

A burst is classified as an XRF when the Softness Ratio (SR) between the fluences in the 2.0-30.0 keV band to the 30.0-400.0 keV band is greater than 1 (Lamb & Graziani 2003). A burst whose SR is between 1 and 0.32 is classified as XRR, and included in the XRF sample by D’Alessio et al. (2006). Because the SWIFT (Gehrels et al. 2005) BAT instrument (Barthelmy et al. 2005), which provide the trigger condition, has a narrower energy band (15-150 keV), we cannot access to SR directly. This narrow range also imply that the characteristic energy of the Band function can lie outside the detection band in several cases. In fact, most of the SWIFT prompt emission spectra are well fit by a simple power law (Zhang et al. 2006), as one can expect in such a case. To build our XRF sample, we thus need to translate the condition on SR into a condition on the observed power law index. D’Alessio et al. (2006) found that the mean values for their XRF sample were $E_p = 36$ keV, $\alpha = 1.2$, $\beta = 1.7$. We conservatively selected in our sample only those events satisfying the conditions $E_p < 15$ keV and $\beta > 2$, that give the condition $SR > 1$.

We constructed our sample using events observed by SWIFT until the 12th of May 2006 (included). We retrieved the best fit power law indexes of the prompt spectra from the SWIFT official web page¹. Twenty-one events were classified as XRFs using our criterion. We made a systematic analysis of the XRT observations of those events (details are given in Galli et al., in preparation). In this letter, we restrict our sample to bursts with known redshift (9 XRFs, 43 % of the total sample). These events are compared to SWIFT GRBs with known redshift for which a published XRT light curve is available. Most of these bursts came from the work of O’Brien et al. (2006). Tables 1 and 2 list our samples of XRFs and GRBs respectively, together with the 2.0-10.0 keV fluxes (expressed 40 ksec after the burst, observer frame) and luminosities (expressed 20 ksec after the burst, rest frame). We compute this latter value using the flux observed at $20 \times (1 + z)$ ksec, applying the k-correction using the spectral indexes listed in Galli et al. (in preparation).

The mean redshifts of SWIFT XRFs and GRBs are $\langle z_{XRF} \rangle = 1.40$, $\sigma = 1.06$ and $\langle z_{GRB} \rangle = 2.05$, $\sigma = 1.16$ respectively. The logarithmic mean fluxes of our two samples are $\langle \text{Log} F_{XRF,13} \rangle = 0.6 \pm 0.2$ and $\langle \text{Log} F_{GRB,13} \rangle = 0.8 \pm 0.2$. Correcting for distance effects, we obtain a logarithmic mean luminosity of

Table 2. SWIFT GRB sample. We report the redshift, the prompt spectral parameter β , the 2.0-10.0 keV flux 40 ksec after the burst (observer frame) and the 2.0-10.0 keV luminosity 20 ksec after the burst (rest frame). GRB 050408 was detected by HETE-2; it has $E_p = 18$ keV, thus classifying this event as GRB using our criterion. It is however more likely an X-Ray Rich event rather than a normal GRB.

GRB name	Redshift	β	X-ray flux 10^{-13} erg s $^{-1}$ cm $^{-2}$ (40 ksec, observer frame)	X-ray luminosity 10^{44} erg s $^{-1}$ (20 ksec rest frame)
050525A	0.606	1.06	8.51	2.1
050318	1.44	1.31	5	2.5
050223	0.5915	1.84	0.691	0.2
050505	4.27	1.40	15.1	111
050126	1.29	1.33	0.375	0.5
050401	2.9	1.41	20.6	119
050408	1.236	(HETE)	8.88	14.4
051111	1.549	1.32	2.52	7.2
050730	3.97	1.52	38	77.2
060124	2.3	1.89	60.3	307
050603	2.281	1.17	12.2	38.8
050802	1.71	1.55	5.98	12.4
050922C	2.198	1.35	2.08	14.7
050820A	2.612	1.21	41.25	255
050908	3.35	1.86	0.2071	193
050803	0.422	1.40	12.85	1.1

$\langle \text{Log} L_{XRF,44} \rangle = 0.34 \pm 0.55$ and $\langle \text{Log} L_{GRB,44} \rangle = 1.18 \pm 0.25$. Note that XRF 060218 has a very low luminosity (see Fig. 1 and Table 1). Excluding this event we obtain a mean luminosity $\langle \text{Log} L_{XRF,44} \rangle = 0.77 \pm 0.37$, lower by a factor of 2.58 compared to the mean GRB luminosity.

3. The high distance hypothesis

The softness of XRFs compared to GRBs can be accounted for by assuming that XRFs are at higher ($z > 5$) distance than GRBs (Heise et al. 2001). No SWIFT XRFs with known redshift is at high distance (see Fig. 1), thus implying that this hypothesis cannot account for all XRFs. However, some of them could indeed be high redshift GRBs. A distant event would have no optical afterglow emission because of the Lyman break redshifted in the optical band (Fruchter 1999). If a significant fraction of XRFs are high distance GRBs, one may roughly expect a greater fraction of *dark* events among XRFs compared to GRBs (De Pasquale et al. 2003). However, in our complete sample of 21 XRFs, twelve (57.1% of the sample) have an optical afterglow (to be compared to the 48.7% of SWIFT GRBs that have an optical afterglow)². This would argue against the fact that a significant fraction of our XRF sample are high redshift GRBs.

However, one may wonder if this is due to any selection effect, since the detection threshold of the BAT instrument changes depending on the observed E_p value of the burst. The BAT sensitivity threshold to an XRF with $E_p \sim 15$ keV is ~ 3 ph cm $^{-2}$ s $^{-1}$ in the 1.0-1000.0 keV band (Band 2006), while it is ~ 1 ph cm $^{-2}$ s $^{-1}$ in the same band for a GRB with $E_p \sim 150$ keV. We have computed the minimum peak luminosity needed for an XRF with an observed $E_p \sim 15$ keV in order to trigger the BAT instrument as a function of the redshift, and compared it to the measured peak luminosity of our sample.

¹ see http://swift.gsfc.nasa.gov/docs/swift/archive/grb_table/

² see <http://www.mpe.mpg.de/jcg/grbgen.html>

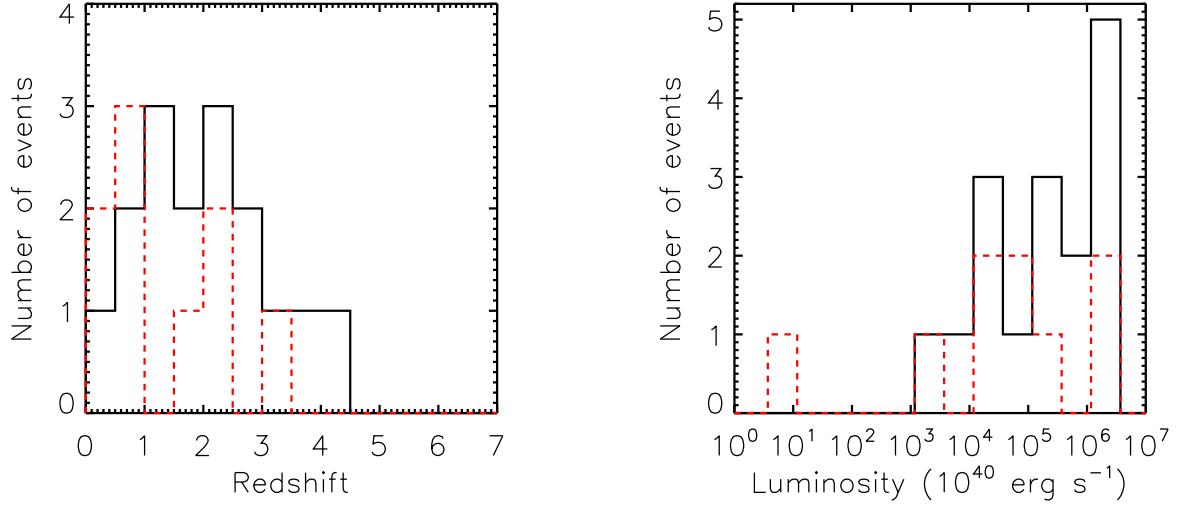


Fig. 1. The redshift (left) and luminosity (right) distributions of XRFs (dashed red line) and GRBs (solid black line). Luminosities are given at 20 ks in the burst frame.

Figure 2 presents the result. One can clearly see that XRFs are too dim to be detected by SWIFT at high redshift. While several events are significantly above the calculated limit, an XRF that presents the mean characteristics of our sample could be detected only up to $z \sim 2$. Only a bright XRF could be observed up to $z \sim 5 - 6$. In fact, using the Amati relation (Amati 2006) to compute the peak luminosity of a burst with an observed E_p of 2 or 15 keV, and a duration of 20 seconds (rest frame), these events cannot be observed at redshift larger than ~ 0.5 and ~ 2 respectively. All of this imply that our sample is biased toward nearby and intermediate redshifts. This explains why we observe a mean redshift of XRFs lower than the GRB one. We stress that this effect is only due to the detection efficiency bias. Note however that SWIFT can indeed detect high distance GRBs, but these events have a very high intrinsic \tilde{E}_p value which make them classified as GRBs rather than XRFs.

4. The off-axis hypothesis

D’Alessio et al. (2006) have tested three different hypotheses for the jet geometry : the Universal Power law (UP), the Quasi-Universal Gaussian (QUG), and the Off-axis Homogeneous (OH) jets. These models involve a typical core size of the jet θ_c , and predict a viewing off-axis angle (θ_v) for a given intrinsic \tilde{E}_p value. Using this value of θ_v , one can then compute the afterglow emission light curve. Different \tilde{E}_p values imply different viewing angles and thus different afterglow emission light curves for XRFs and GRBs. Large differences are expected at early times ($\lesssim 1$ day, rest frame) with the luminosity decreasing when θ_v increases. Hence, one can compute R_X , a GRB to XRF afterglow emission luminosity ratio at a given time (see D’Alessio et al. 2006, for details). The \tilde{E}_p values for the events of our samples are unknown. Using our criterion ($E_p = 15$ keV) and the mean XRF redshift, we obtain $\langle \tilde{E}_{p, XRF} \rangle < 36$ keV. Six XRFs of our sample are listed in Zhang et al. (2006). Using their estimates, we have $\langle \tilde{E}_{p, XRF} \rangle = 64.8$ keV. Note that this value is higher than the one implied by our assumption (see Galli et al. in preparation for a complete discussion); however this value is still lower than that of D’Alessio et al. (2006), $\langle \tilde{E}_{p, XRF, XRR} \rangle = 136$ keV. This latter value is higher because of the inclusion of XRRs in their

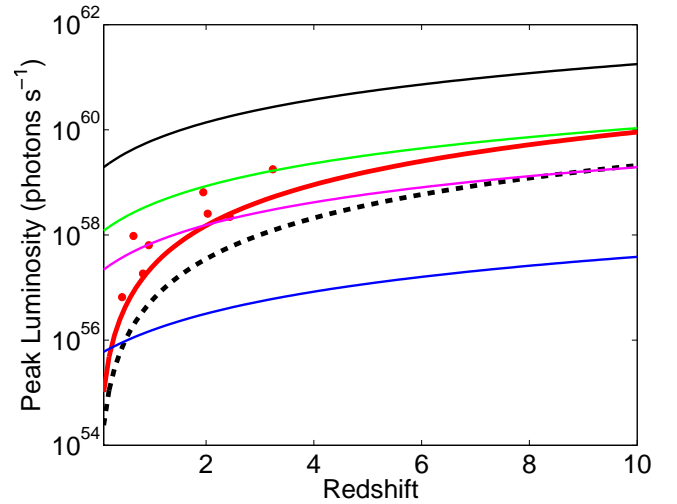


Fig. 2. The selection effects. The solid red and dashed black lines represent the detection threshold of the SWIFT BAT instrument for an XRF with an observed $E_p = 15$ keV and a GRB with an observed $E_p = 150$ keV respectively. The red points are the peak luminosity of our sample. The other solid lines represent the peak luminosity expected from the Amati relation to produce a burst with an E_p of 2 keV (blue line), 15 keV (purple line), 36 keV (green line) and 150 keV (black line) in the observer frame. See the electronic version for colors.

sample. As for GRBs, using again the estimates of Zhang et al. (2006) for our GRB sample, we derive $\langle \tilde{E}_{p, GRB} \rangle \sim 398$ keV, in agreement with the BeppoSAX result of $\langle \tilde{E}_{p, GRB} \rangle \sim 410$ keV (D’Alessio et al. 2006).

Our sample of XRFs has a lower mean value of $\langle \tilde{E}_p \rangle$ compared to that of D’Alessio et al. (2006). Thus, the values of R_X quoted in D’Alessio et al. (2006) are lower limits for our sample. Assuming a core size of the jet large enough to account for the typical jet break time (a few days, De Pasquale et al. 2006; Gendre et al. 2006), one should observe a ratio larger than ~ 20 ,

~ 10 and ~ 1.2 for the UP, QUG and OH models respectively, when expressed 20 ksec after the burst (rest frame).

We observe $R_X = 2.6^{+2.6}_{-2.0}$. Because we now have access to the luminosity distribution rather than the flux one (thus removing the uncertainties pointed out by D'Alessio et al. 2006), we can clearly rule out large values of R_X . We thus confirm the claim of D'Alessio et al. (2006) that an homogeneous jet with opening angle $\theta_j \approx 6.1^\circ$ is the only one that can account for the observed R_X . Anyway a jet opening angle of 6° fails to explain the distribution of prompt emission properties. In fact, population synthesis simulations of the bursts performed by Lamb et al. (2005) showed that, in order to reproduce the observed distribution of E_{peak} , E_{iso} and fluence of a sample of GRBs plus XRFs detected by BeppoSAX and HETE-2, a mean opening angle $\theta_j \sim 0.5^\circ$ is required. Furthermore, an OH jet with a such small mean opening angle implies a GRB/SN ratio of about 1. But, as shown by Berger et al. (2003) and Soderberg et al. (2004), no evidence for relativistic jet was found in SNe, thus constraining the GRB/SN fraction to be very low. Consequently, this jet model is also not favored by the global data.

5. Discussion and conclusions

In this Letter, we have investigated the nature of XRFs, using a sample of events observed by SWIFT. As explained in Section 3, the high distance hypothesis might hold for a very few (if any) of the soft events. In fact, SWIFT XRFs cannot be distant events due to a selection effect of the BAT instrument. The access to the luminosity distribution provided for the first time by SWIFT allowed us to strongly constrain the off-axis scenario. We found that for an suitable jet opening angle value an OH model is the only one that could account for the XRF X-ray afterglow luminosities. However, the same jet opening angle fails to account for prompt properties of XRFs versus GRBs.

One could put into question the core size of the jet, not well constrained yet. A lower value of the core size may reduce significantly the luminosity ratio expected in case of the UP model, thus making this model still plausible. However, the presence and occurrence time of temporal breaks in the afterglow emission light curve are key arguments to constrain the value of the core size of the jet, and will be discussed in Galli et al. (in preparation). A final possibility is that XRFs are produced by an inefficient fireball or a sub-energetic progenitor. For instance, in the context of internal shocks, XRFs may be produced by relativistic outflows with a low contrast in the Lorentz factor distribution, giving an efficiency of energy dissipation lower than in GRBs (Barraud et al. 2003). In an external shock scenario, a fireball with a low Lorentz factor can account for the low E_p value observed (Dermer 1999). This can be produced by a fireball with a high baryon load or a sub-energetic progenitor. In that latter case, the model is however challenged to produce an under-luminous prompt emission but an XRF afterglow luminosity similar to the GRB one.

Acknowledgements. Thanks are due to E. M. Rossi for useful comments. We would also like to thank the anonymous referee for her/his very constructive report. BG acknowledge support from COFIN grant 2005025417.

References

- Amati, L., 2006, MNRAS, 372, 233
 Band, D., Mateson, J., Ford, L., et al., 1993, ApJ, 413, 281
 Band, D.L., 2006, ApJ, 644, 378
 Barraud, C., Oliver, J. F., Lestrade, J.P., et al., 2003, A&A, 400, 1021
 Barraud, C., Daigne, F., Mochkovitch, R., & Atteia, J.L., 2005, A&A, 40, 809
 Barthelmy, S.D., Barbier, L.M., Cummings, J.R., et al., 2005, Space Science Review, 120, 143
 Berger, E., Kulkarni, S.R., Frail, D.A., & Soderberg, A.M., 2003, ApJ, 599, 408
 D'Alessio, V., Piro, L., & Rossi, E.M., 2006, A&A, 460, 653
 Dermer, C. D., Chiang, J., & Bottcher, M., 1999, ApJ, 513, 656
 Eichler, D., & Levinson, A., 2004, ApJ, 614, L13
 Fruchter, A.S., 1999, ApJ, 516, 683
 Gendre, B., Corsi, A., & Piro, L., 2005, A&A, 455, 803
 Gehrels, N., Chincarini, G., Giommi, P., et al., 2005, ApJ, 611, 1005
 Heise, J., in't Zand, J., Kippen, R.M., & Woods, P.M., in Proc. 2nd Rome Workshop: Gamma-Ray Bursts in the Afterglow Era, 2001, eds E. Costa, F. Frontera, J. Hjorth (Berlin:Springer-Verlag), 16
 Lamb, D.Q., & Graziani, C., 2003, AAS, 202, 450
 Lamb, D.Q., Donaghy, T.Q., & Graziani, C., 2005, ApJ, 620, 355
 O'Brien, P.T., Willingale, R., Osborne, J., et al., 2006, ApJ, 647, 1213
 De Pasquale, M., Piro, L., Perna, R., et al., 2003, ApJ, 592, 1018
 De Pasquale, M., Piro, L., Gendre, B., et al., 2005, A&A, 455, 813
 Ramirez-Ruiz, E., & Lloyd-Ronning, N.M., 2002, New Astron., 7, 197
 Sakamoto, T., Lamb, D.Q., Kawai, N., et al., 2005, ApJ, 629, 311
 Soderberg, A.M., Frail, D.A., & Wieringa, M.H., 2004, ApJ, 607, L13
 Toma, K., Yamazaki, R., & Nakamura, T., 2005, ApJ, 635, 481
 Yamazaki, R., Ioka, K., & Nakamura, T., 2002, ApJ, 571, 31
 Yamazaki, R., Ioka, K., & Nakamura, T., 2003, ApJ, 593, 941
 Yamazaki, R., Ioka, K., & Nakamura, T., 2004, ApJ, 606, 33
 Zhang, B., Dai, X., Lloyd-Ronning, N., & Meszaros, P., 2004, ApJ, 601, 119
 Zhang, B., Liang, E., Page, K.L., et al., 2007, ApJ, 655, 989

List of Objects

- '060512' on page 2
 '060218' on page 2
 '060108' on page 2
 '051016B' on page 2
 '050824' on page 2
 '050416A' on page 2
 '050406' on page 2
 '050319' on page 2
 '050315' on page 2
 'GRB 050408' on page 2
 '050525A' on page 2
 '050318' on page 2
 '050223' on page 2
 '050505' on page 2
 '050126' on page 2
 '050401' on page 2
 '050408' on page 2
 '051111' on page 2
 '050730' on page 2
 '060124' on page 2
 '050603' on page 2
 '050802' on page 2
 '050922C' on page 2
 '050820A' on page 2
 '050908' on page 2
 '050803' on page 2